Proceedings of the 9th U.S. National and 10th Canadian Conference on Earthquake Engineering
Compte Rendu de la 9ième Conférence Nationale Américaine et
10ième Conférence Canadienne de Génie Parasismique
July 25-29, 2010, Toronto, Ontario, Canada • Paper No 1562

EFFECT OF GROUND MOTION SUITES ON THE SEISMIC FRAGILITY OF A THREE-SPAN CONTINUOUS STEEL GIRDER BRIDGE

K. Ramanathan[1], T. Wright[1], R. DesRoches[2] and J. E. Padgett[3]

ABSTRACT

The seismic hazard in the Central and Southeastern United States has gained widespread attention in recent years. Due to the lack of available recorded strong ground motions in the region, the earthquakes used in many analytical studies of the region's infrastructure have typically been synthetic. This paper investigates the difference in the response of a bridge typical to this region due to two different suites of ground motions. The first suite is comprised of synthetic earthquakes from the New Madrid Seismic Zone and the second suite of ground motions is comprised primarily of recorded ground motions from previous events in southern California. This study focuses on developing two sets of fragility curves for a three-span continuous steel girder bridge using 3-D analytical models and nonlinear time-history analyses. Comparing the component and system fragility curves allows for an evaluation of the vulnerability of the bridge subject to the two distinct hazards.

Introduction

The New Madrid and Wabash Valley seismic zones are located along the Mississippi River and stretch from Arkansas and Tennessee north to Indiana and Illinois. During the years of 1811 and 1812, four of the largest earthquakes to have occurred in the continental United States took place in a matter of three months in this region. Three of the earthquakes are estimated to have had magnitudes ranging from 7.8 to 8.1 on the Richter scale. While there have not been earthquakes of magnitude 6.0 or greater in over a hundred years, the threat of large earthquakes in the future exists. According to some researchers, there is a 90% probability that a magnitude 6 or 7 earthquake will occur within the next fifty years (Hildenbrand et al. 1996). Until the early 1990's, there were no modern seismic design codes in the region, so the current stock of highway bridges, which has an average age of more than 38 years old (Wright et al. 2009), is particularly vulnerable to sustaining excessive and widespread damage during a repeat large seismic event. As knowledge of the seismic hazard in the central and southeastern United

[1] Graduate Research Assistant, School of Civil & Environmental Engineering, Georgia Institute of Technology, Atlanta, GA 30332
[2] Professor & Associate Chair, School of Civil & Environmental Engineering, Georgia Institute of Technology, Atlanta, GA 30332
[3] Assistant Professor, Dept.of Civil & Environmental Engineering, Rice University, Houston, TX 77005

States (CSUS) has grown, the need for seismic evaluations of structural systems in the region has been highlighted.

The scarcity of empirical data of earthquake damage in the CSUS requires that risk assessments in the region be analytically based. Fragility curves represent the probability of exceeding predetermined damage states of a structure conditioned against a ground motion intensity measure and have become an important tool in assessing the seismic vulnerability of highway bridges in regions of moderate seismicity. Analytical fragility curves have been formulated through a variety of means, including elastic spectral response (Jernigan and Hwang 2002), nonlinear static analysis (Mander and Basoz 1999), and nonlinear time history analyses (Nielson and DesRoches 2007; Mackie and Stojadinovic 2001; Karim and Yamazaki 2003). Although it is the most computationally intensive, performing nonlinear time history analyses is typically the most reliable method of developing these fragility functions. Arising from a lack of recorded strong ground motions in the CSUS, recent analytically based fragility curves for bridges in the CSUS have typically been generated using synthetic ground motions (Hwang et al. 2000; Choi et al. 2004; Nielson and DesRoches 2006). The work presented herein subjects a deterministic bridge to two suites of ground motions – one from the New Madrid Seismic Zone (synthetic) and one from Los Angeles (recorded and synthetic) – and corresponding system fragility curves are developed for both cases. By comparing the system fragility curves for the two earthquake portfolios, this paper will investigate the difference in seismic vulnerability of a deterministic bridge due to two distinct seismic hazards, one in the central US (synthetic), and one on the west coast (primarily recorded).

Deterministic Bridge Characteristics

The bridge that is chosen for the analytical modeling is a ‘typical’ three-span continuous steel girder bridge. This bridge type, as its name suggests, has continuous steel girders over the bents. The three equal length spans are 30.3 m long (100 ft) and 15 m wide (49.5 ft). The spans are supported by 520 mm (20.5 in) tall fixed steel bearings at one end and by 520 mm (20.5 in) tall steel rocker bearings at the opposite end. The two bents are each supported by three reinforced circular concrete columns that have a diameter of 900 mm (36 in) and a height of 4.6 m (15 ft). The columns are reinforced longitudinally with 12- #29 bars and are reinforced transversely with #13 bars at 305 mm (12 in) on center. The two bent beams are 1.07 m (42 in) wide and 1.22 m (48 in) deep with 6- #29 and 9- #29 reinforcing bars placed in the top and bottom respectively. There are also 2-# 16 reinforcing bars placed longitudinally along either side of the section and #16 stirrups spaced at 305 mm (12 in). A detailed schematic of the bridge is shown in Figure 1. It should be noted that while there are a number of other bridges that could be modeled, the selection of the bridge itself is not of key importance to the goals of this study. Ultimately a comparison of the bridge response due to the two different suites of ground motions is desired.

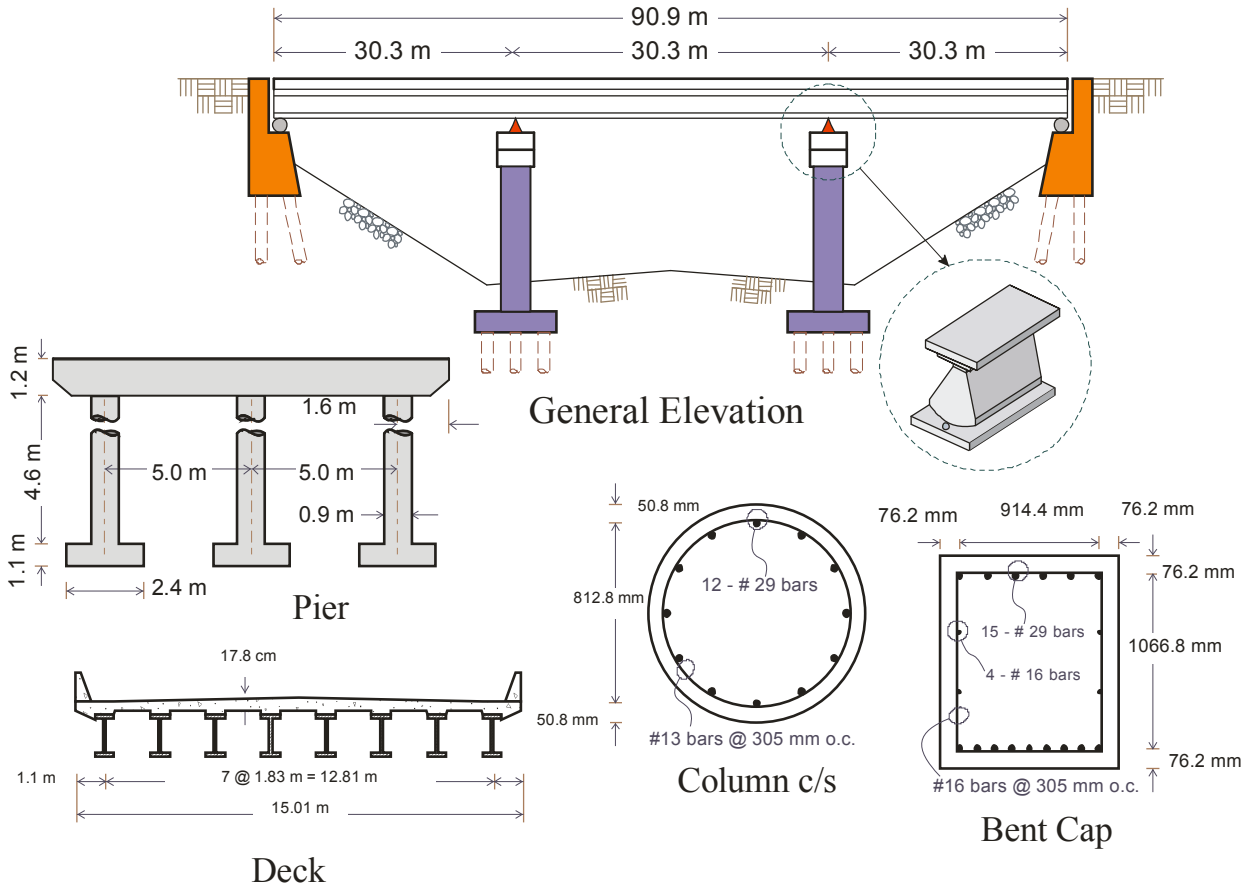

Figure 1. Basic layout of the bridge

Analytical Modeling of the Bridge

A detailed analytical model that accounts for material and geometric nonlinearities in the bridge is developed in the OpenSEES platform (McKenna and Fenves 2005). The columns and bent caps are modeled using fiber sections. These fiber sections directly model the longitudinal steel, and can represent the transverse reinforcing by modeling different properties for the confined versus unconfined concrete. The effect of the confinement is determined using the confined concrete model developed by Mander et al. (1988). Because the superstructure of the bridge will remain linearly elastic during an earthquake event, the bridge deck is modeled using a single girder (spine) model. Elastic beam-column elements are used to model the deck, and the dynamic deck mass is appropriately lumped at the nodes along the centerline of the bridge. The steel bearings are modeled based on experimental tests performed by Mander et al. (1996). By modeling the bearings with zero-length elements that combine the behavior of a steel material in parallel with a hysteretic material, the complex behavior of the bearings is accurately modeled. Following the analytical modeling method outlined in Nielson and DesRoches (2007), the abutments and abutment piles are modeled by a combination of linear and nonlinear springs in parallel. The analytical model used is illustrated in Figure 2.

The orthogonal components of each ground motion are applied to the bridge model simultaneously and a complete nonlinear time history analyses is performed. One component of

the ground motion is applied to the bridge along its principal longitudinal axis and the other orthogonal component is applied in the transverse direction. By applying two dimensional ground motions to the three-dimensional bridge model, a more realistic representation of the seismic demand on the bridge is observed. All material and geometric variabilities are ignored in this study so that a better comparison of the ground motion suites and their influence on the bridge vulnerability may be investigated.

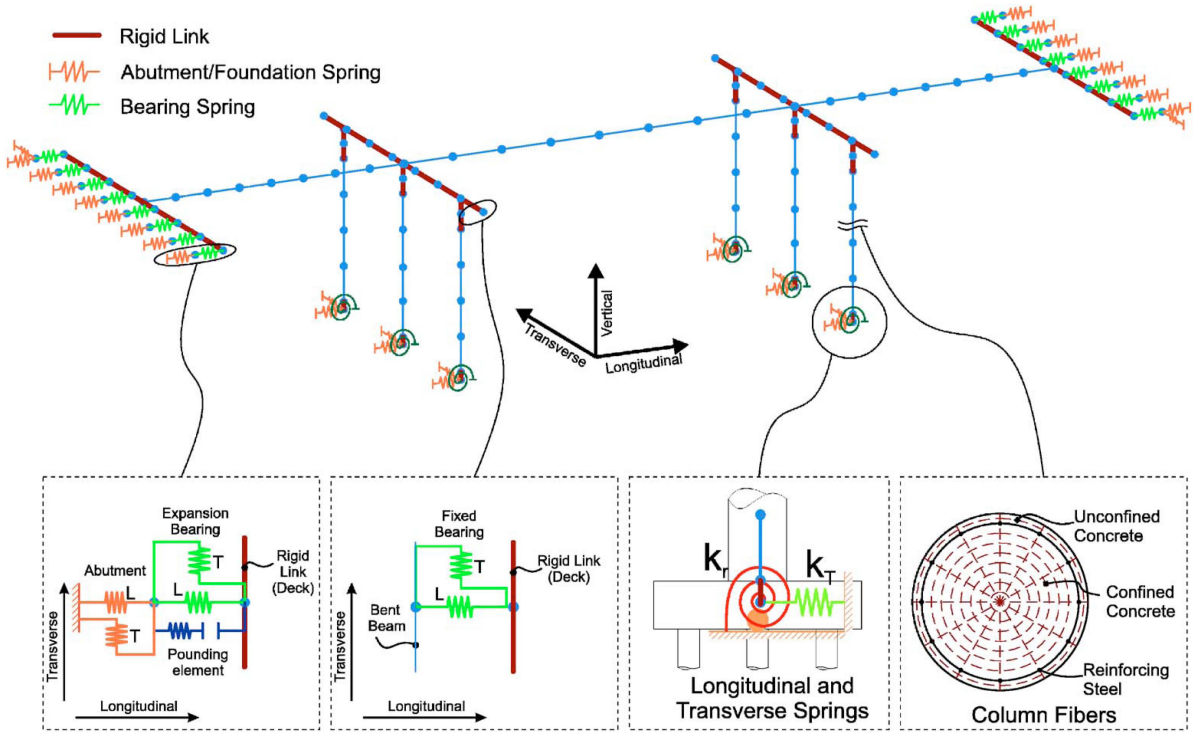

Figure 2. Schematic of important modeling considerations (Nielson and DesRoches 2007)

Ground Motion Suites and Characteristics

While selecting ground motion suites, the objective was to use two well established suites of ground motions which are commonly used in performing seismic analyses of structures in the CSUS and on the west coast. The west coast ground motion suite used is the SAC suite for Los Angeles. This set of ground motions contains thirty pairs of orthogonal ground motion records. The probabilities of exceedance for the thirty ground motions are evenly split between 2%, 5%, and 10% in 50 yrs. The ground motions range in PGA from 0.14g to 1.28g, and have epicentral distances ranging from 1km to 107km.

For the New Madrid region, a suite of forty-eight synthetic ground motions is used. These forty-eight ground motions are selected from a portfolio of 220 scenario earthquakes developed for the Memphis, TN region by Rix and Fernandez. The magnitudes of the synthetic earthquakes range from 5.5 to 7.5, while the epicentral distances range from 10km to 100km. These ground motions are decomposed into two orthogonal components using the procedure developed by Baker and Cornell (2006). The geometric mean of the PGA values of the orthogonal components

varies between 0.03g and 0.74g. The mean response spectra for the two earthquake portfolios are plotted in Figure 3.

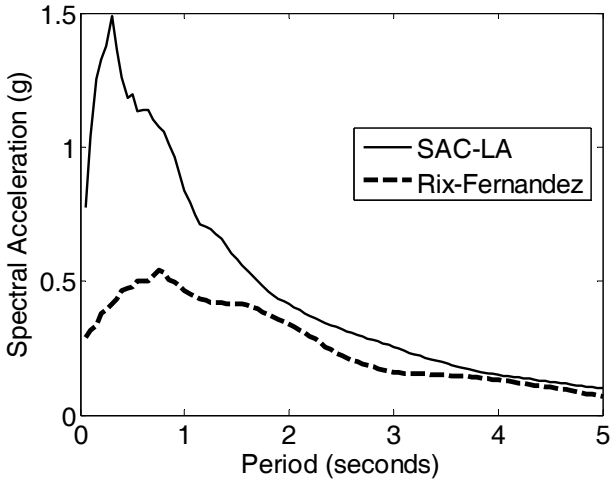

Figure 3. Mean response spectra for the two ground motion suites (5% damping)

PSDMS and Fragility Curve Formulation

Fragility curves in this study are based on full nonlinear time history analyses which aid in the estimation of the seismic demand placed on the bridges and their components. Fragility curves consider the probability that the seismic demand (D) placed on the structure exceeds the capacity (C) conditioned on a chosen intensity measure (IM) representative of the seismic loading. D and C are assumed to follow lognormal distributions and the probability of reaching or exceeding a specific damage state can be estimated using the standard normal cumulative distribution function, defined as,

$$P[D > C/IM] = \Phi\left(\frac{\ln(S_d / S_c)}{\sqrt{\beta_{d/IM}{}^2 + \beta_c{}^2}}\right) \quad (1)$$

where, S_d is the median estimate of the demand as a function of IM, S_c is the median estimate of the capacity, $\beta_{d/IM}$ is the dispersion or logarithmic standard deviation of the demand conditioned on the IM, β_c is the dispersion of the capacity and $\Phi(\cdot)$ is the standard normal cumulative distribution function. Equation (1) can be evaluated by developing a probability distribution for demand conditioned on a chosen IM, commonly known as the probabilistic seismic demand model (PSDM), and convolving it with the capacity distribution. The median demand, S_d can be expressed as a power function (Cornell et al. 2002):

$$S_d = a(IM)^b \quad (2)$$

where, a and b are regression coefficients. A linear regression of the demand – IM pairs determines the values of a and b. A set of analytical 3-D models is subjected to a suite of n ground motions and in each case the peak demand measures (such as column curvature ductility,

bearing and abutment deformations) are recorded. The dispersion of the demand conditioned on IM is given by,

$$\beta_{d/IM} = \sqrt{\frac{\sum_{i=1}^{n}\left(\ln d_i - \ln a(IM)^b\right)^2}{n-2}} \tag{3}$$

The bridge is then analyzed for each ground motion using non-linear time history analysis and the maximum component responses are recorded in each case. The components considered in this study are columns, steel fixed and expansion (rocker) bearings and abutments (both active and passive as well as transverse). This study formulates fragility curves for the bridge for four different ground intensity measures: peak ground acceleration (PGA), spectral acceleration at the geometric mean of the first two periods ($S_{a\text{-}gm}$), spectral acceleration at the first natural period ($S_{a\text{-}T1}$) and spectral acceleration at the second natural period ($S_{a\text{-}T2}$). The most efficient parameters investigated are PGA and $S_{a\text{-}gm}$, and the fragility curves considering those two intensity measures are the only two presented herein. Fig. 4 shows demand plots for the expansion bearings in the longitudinal direction of PGA and $S_{a\text{-}gm}$ respectively.

The summary of the PSDMs for all components of the bridge analyzed with the Rix-Fernandez suite and SAC-Los Angeles suite as functions of PGA are given in Table 1, where R^2 is the coefficient of determination indicating the accuracy of fit. From the R^2 values in Table 1, it is evident that the transformed data for the Rix-Fernandez ground motion has a much better linear fit than the corresponding data from the SAC-Los Angeles suite.

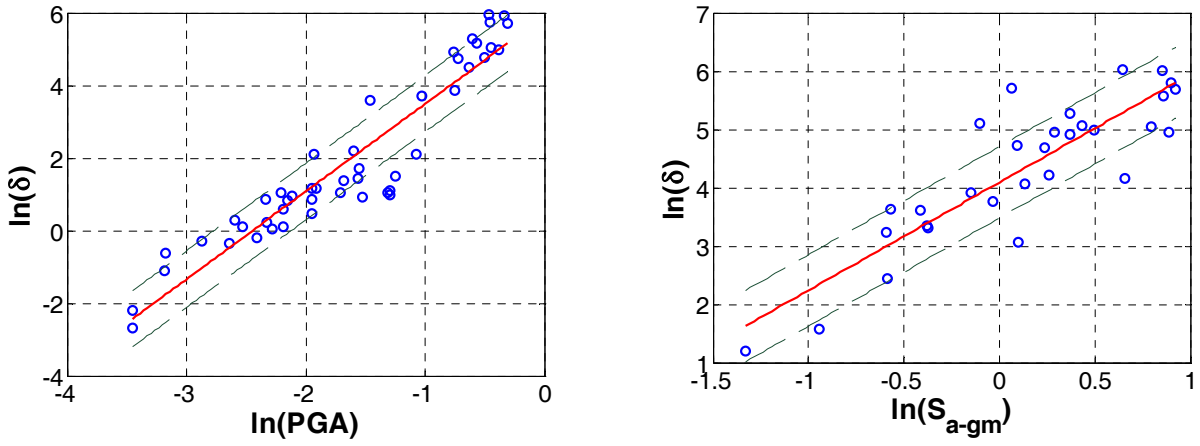

Figure 4. PSDMs for lateral displacement demand of steel expansion (rocker) bearing a) as a function of PGA for Rix-Fernandez suite and b) as a function of $S_{a\text{-}gm}$ for the SAC-Los Angeles suite

Table 1. PSDM parameter estimates for various components (based on PGA)

Component	Rix-Fernandez				SAC-Los Angeles			
	a	b	$\beta_{d/PGA}$	R^2	a	b	$\beta_{d/PGA}$	R^2
Column	3.79	2.11	0.63	0.90	3.11	1.78	0.82	0.60
Fixed steel bearing-longitudinal	0.55	0.88	0.42	0.78	-.07	0.22	0.12	0.53
Fixed steel bearing-transverse	4.64	2.42	1.10	0.80	4.66	2.45	0.80	0.75
Steel rocker bearing-longitudinal	5.88	1.28	0.50	0.84	5.28	0.72	0.33	0.60
Steel rocker bearing-transverse	5.91	2.42	0.78	0.89	5.52	1.99	0.56	0.80
Abutment - passive	5.12	2.62	1.30	0.76	4.68	2.80	1.59	0.50
Abutment - active	0.51	0.53	0.24	0.79	0.20	0.23	0.15	0.45
Abutment - transverse	2.25	0.69	0.27	0.84	1.84	0.14	0.10	0.39

Component Limit States

The components considered in this study are columns, fixed and expansion bearings and abutments (both active and passive).The component limit states are also assumed to be lognormally distributed. The median, S_c and the dispersion, β_c values of the limit states are obtained from experimental results. The study uses four damage states, slight, moderate, extensive and complete, comparable to those found in HAZUS-MH. Table 2 below summarizes the limit state values for the various components. Further details regarding the limit states can be found in the work by Nielson and DesRoches (2007).

Table 2. Bridge component limit states

Component	Slight		Moderate		Extensive		Complete	
	S_c	β_c	S_c	β_c	S_c	β_c	S_c	β_c
Column (μ)	1.29	0.59	2.10	0.51	3.52	0.64	5.24	0.65
Fixed steel bearing-long (mm)	6	0.25	20	0.25	40	0.47	186.6	0.65
Fixed steel bearing-(trans) (mm)	6	0.25	20	0.25	40	0.47	186.6	0.65
Steel rocker bearing-(long) (mm)	37.4	0.60	104.2	0.55	136.1	0.59	186.6	0.65
Steel rocker bearing-(trans) (mm)	6	0.25	20	0.25	40	0.47	186.6	0.65
Abutment - passive (mm)	37.0	0.46	146.0	0.46	N/A	N/A	N/A	N/A
Abutment - active (mm)	9.8	0.70	37.9	0.90	77.2	0.85	N/A	N/A
Abutment - trans (mm)	9.8	0.70	37.9	0.90	77.2	0.85	N/A	N/A

Component and system fragility curves

Having estimated the demand and capacity parameters, the fragility curves for various bridge components can be obtained based on the formulation given in Equation (1). The system level fragilities are formulated using the joint probabilistic seismic demand model (JPSDM) as outlined in the work by Nielson and DesRoches (2006). The JPSDM is developed by assessing the demands placed on each component (marginal distribution) through a regression analysis as in the case of PSDMs. The covariance matrix is assembled by estimating the correlation

coefficients between the demands placed on the various components. A Monte Carlo simulation is then used to compare realizations of the demand (using the JPSDM defined by a conditional joint normal distribution) and statistically independent component capacities to calculate the probability of system failure across a range of intensity measures and for each damage state. This procedure is repeated for each level of IM for each of the damage states. Regression analysis is used to estimate the lognormal parameters, median, λ and standard deviation or dispersion, ζ, which characterize the bridge system fragility.

Table 3. Summary median and dispersion values (in g) of component fragilities using PGA as the indexed intensity measure.

		Slight		**Moderate**		**Extensive**		**Complete**	
Component	**GM**	λ_c	ζ_c	λ_c	ζ_c	λ_c	ζ_c	λ_c	ζ_c
Column	Rix	0.186	0.409	0.235	0.384	0.300	0.425	0.363	0.429
	LA	0.201	0.568	0.264	0.543	0.353	0.585	0.441	0.588
Fixed bearing (longit.)	Rix	N/A	N/A	N/A	N/A	N/A	N/A	N/A	N/A
	LA	N/A	N/A	N/A	N/A	N/A	N/A	N/A	N/A
Fixed bearing (transv.)	Rix	0.307	0.456	0.506	0.456	0.674	0.486	1.278	0.520
	LA	0.311	0.343	0.508	0.343	0.674	0.380	1.263	0.421
Expansion bearing (longit.)	Rix	0.171	0.609	0.381	0.578	0.470	0.600	0.601	0.639
	LA	0.102	0.948	0.417	0.885	0.603	0.931	0.933	1.008
Expansion bearing (transv.)	Rix	0.182	0.338	0.299	0.338	0.398	0.377	0.754	0.419
	LA	0.153	0.309	0.280	0.309	0.397	0.369	0.863	0.432
Abutment (passive)	Rix	0.562	0.528	0.949	0.528	1.977	0.497	1.977	0.497
	LA	0.683	0.590	1.115	0.590	2.213	0.567	2.213	0.567
Abument (active)	Rix	N/A	N/A	N/A	N/A	N/A	N/A	N/A	N/A
	LA	N/A	N/A	N/A	N/A	N/A	N/A	N/A	N/A
Abutment (transv.)	Rix	1.036	1.083	N/A	N/A	N/A	N/A	N/A	N/A
	LA	N/A	N/A	N/A	N/A	N/A	N/A	N/A	N/A

The fragility curves for the bridge components are not explicitly shown; however, Table 3 summarizes the component median, λ_c, and component dispersion values, ζ_c, for the component fragilities due to both portfolios of ground motions (considering PGA as the intensity measure). For the components that were found to be not seismically vulnerable – defined as having median value larger than 4.0 g – the values were replaced with the designation "N/A". Accordingly, it was found that the abutment was typically not vulnerable to sustaining damage actively or in the transverse direction, and the fixed bearing was not vulnerable in the longitudinal direction for either ground motion suite. It is noteworthy that the use of the LA suite

of ground motions led to higher variability of the component fragilities in almost every instance. The Rix and Fernandez ground motions lead to a higher vulnerability in the components in almost every instance, with the only clear exception being the steel expansion bearings in the transverse direction.

Table 4 below summarizes the median and dispersion of the lognormal system wide fragility curves for both suites of ground motions, with the intensity measures being PGA and $S_{a\text{-}gm}$. The fragility curves are plotted for a visual representation in Figure 5, with the solid lines representing the results from the SAC-LA suite and the dashed lines representing the fragility curves due to the Rix-Fernandez suite. From Table 4 and Figure 5, it is apparent that the bridge is more vulnerable to the suite of synthetic CSUS ground motions except for the slight damage state. Again, there is also slightly more variability associated with the west coast ground motions. While PGA as an intensity measure leads to lower variability via the dispersion values, the ratios of dispersion values, **ζ,** to median values, **λ,** are smaller when $S_{a\text{-}gm}$ is the chosen intensity measure.

Table 4. Median and dispersion values for system-wide fragility curves.

	Slight		Moderate		Extensive		Complete	
Intensity measure (IM)	**λ**	**ζ**	**λ**	**ζ**	**λ**	**ζ**	**λ**	**ζ**
SAC- Los Angeles								
PGA (g)	0.081	0.669	0.224	0.452	0.289	0.496	0.399	0.560
$S_{a\text{-}gm}$ (g)	0.154	0.736	0.449	0.462	0.582	0.513	0.803	0.581
Rix and Fernandez								
PGA (g)	0.138	0.423	0.220	0.372	0.272	0.397	0.341	0.421
$S_{a\text{-}gm}$ (g)	0.207	0.515	0.379	0.520	0.476	0.544	0.612	0.602

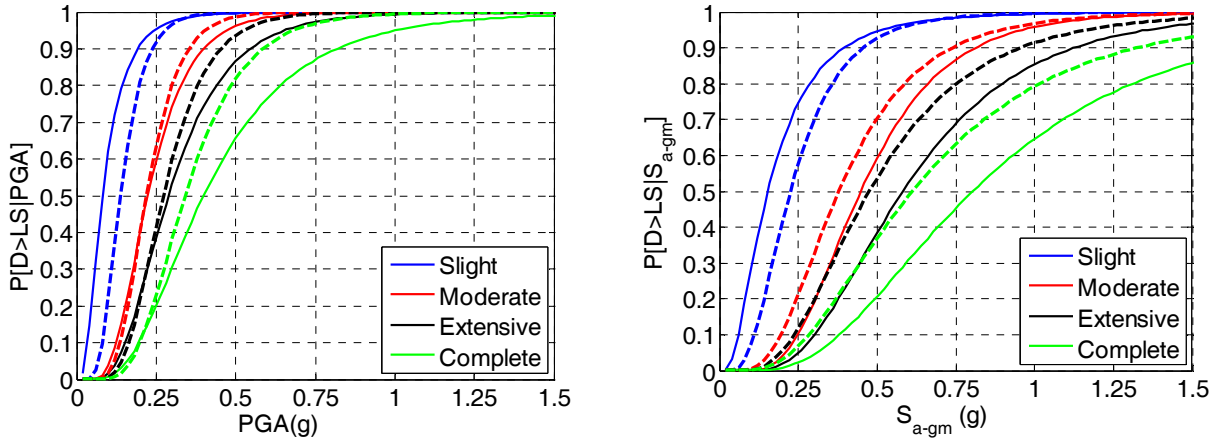

Figure 5. System fragility curve for the two portfolios of ground motions

Conclusions

This paper presents an analytical method for the development of fragility curves of a deterministic three-span continuous steel girder bridge subject to two portfolios of ground motions – one comprised of synthetic earthquakes for the central United States and the other comprised of primarily recorded ground motions for the LA area. The curves are the product of a set of full nonlinear time history analyses of the 3-D analytical model subjected to two orthogonal components of each ground motion. The fragility analyses accounts for the vulnerability of various bridge components including the columns, abutments, and bearings. Furthermore, the component limit states are consistent with those used by Nielson and DesRoches (2007). The fragility analysis shows that the bridge – on both a component and system level – is more seismically vulnerable to the suite of Rix and Fernandez ground motions than the portfolio of Los Angeles ground motions. While this statement may hold true for this single deterministic bridge model, it can be neither generalized nor applied to other bridge types without further studies.

References

Baker, J. and Cornell, A. C. (2006). Which Spectral Acceleration Are You Using?, *Earthquake Spectra*, 22(2).

Choi, E., DesRoches, R., and Nielson, B. (2004). Seismic Fragility of Typical Bridges in Moderate Seismic Zones, *Engineering Structures*, 26(2), 187–199

Cornell, A. C., Jalayer, F., Hamburger, R. O., and Foutch, D. A. (2002). Probabilistic basis for 2000 SAC Federal Emergency Management Agency steel moment frame guidelines, *Journal of Structural Engineering*, 128, 526-532.

Hildenbrand, T.G., Griscom, A., Van Schmus, W.R., and Stuart, W.D. (1996). Quantitative investigations of the Missouri gravity low: A possible expression of a large, Late Precambrian batholith intersecting the New Madrid seismic zone. *Journal of Geophysical Research B: Solid Earth 101 (B10)*, 21921-21942

Hwang, H., Liu, J. B., and Chiu, Y.-H. (2000). "Seismic Fragility Analysis of Highway Bridges." *Report No. MAEC RR-4*, Center for Earthquake Research Information.

Jernigan, J. B. and Hwang, H. (2002). Development of Bridge Fragility Curves. *7th US National Conference on Earthquake Engineering.* Boston, Mass. EERI.

Karim, K. R. and Yamazaki, F. (2003). "A simplified method of constructing fragility curves for highway bridges." *Earthquake Engineering and Structural Dynamics*, 32(10), 1603–1626.

Mackie, K. and Stojadinovic, B. (2001). "Probabilistic Seismic Demand Model for California Bridges." *Journal of Bridge Engineering*, 6(6), 468–480.

Mander, J. B., Priestley, M. J. N., and Park, R., 1988. Theoretical stress-strain model for confined concrete, *Journal of Structural Engineering*, 114(8), 1804-1826.

Mander, J. B., Kim, D. K., Chen, S. S., and Premus, G. J. (1996). "Response of Steel Bridge Bearings to the Reversed Cyclic Loading." *Report No. NCEER 96-0014*, NCEER.

Mander, J. B. and Basoz, N. (1999). "Seismic Fragility Curve Theory for Highway Bridges." *5th US Conference on Lifeline Earthquake Engineering*, Seattle, WA, USA. ASCE.

McKenna, F. and Fenves, G. L. (2005). Open System for Earthquake Engineering Simulation Pacific Earthquake Engineering Research Center, Version 1.6.2.

Nielson, B. G. and DesRoches, R. (2006). Seismic fragility methodology for highway bridges, St. Louis, MO, United States, American Society of Civil Engineers.

Nielson, B. G. and DesRoches, R. (2007). Analytical seismic fragility curves for typical bridges in the central and southeastern United States. *Earthquake Spectra* **23**(3): 615-633.

Wright, T, DesRoches, R., and Padgett, J.E. (2009). Bridge Seismic Retrofitting Practices in the Central and Southeastern US. *Journal of Bridge Engineering*, In Press